コンクリート工学年次論文報告集 9-2 1987

[2115] 境界要素法によるコンクリートのひびわれ進展の解析

BEM ANALYSIS OF CRACK PROPAGATION IN CONCRETE

Masayasu OHTSU* and Yasuo FUKUNAGA**

1. INTRODUCTION

The concept of fracture mechanics has been applied to concrete recently, and crack behaviors in concrete structures are studied. In numerical analyses on crack behaviors, the finite element method (FEM) is extensively employed. Complicated efforts, however, are required in FEM to analyze crack propagation as the nucleation of a new stress-free boundary. Thus, to model a crack in FEM, a fictitious crack model and a smeared crack model are proposed (1).

In contrast to FEM, since no internal points are required in the boundary element method (BEM), an analytical technique does not pose much difficulty to analyze crack propagation as the nucleation of a new stress-free boundary in the arbitrary direction. Consequently, crack propagation in concrete is analyzed by the BEM analysis, and results are compared with experiments.

2. EXPERIMENT

Specimens of four mix proportions are shown in Table 1. These were made of two kinds of air-entrained concrete (specimens AE1 and AE2), steel-fiber-reinforced concrete (SFR), and mortar (MO). In only AE1 specimens, the maximum gravel size was 10 mm. In AE2 and SFR specimens, the maximum gravel size was 20 mm. Steel fibers of dimension 0.5 mm X 0.5 mm X 30 mm were mixed into SFR specimens at 1 % volume ratio. Air entrained agent was added by 4 % of cement weight to AE1, AE2, and SFR specimens. In the table, averaged compressive strength and tensile strength were shown. These were determined from results of three specimens for each mix proportion.

Notched beams of dimension 15 cm X 15 cm X 55 cm and 10 cm X 10 cm X 40 cm were tested. To create a notch at the center of a specimen, a steel plate of 3 mm thichness with an apex angle of 30° was employed in the formwork. In specimens of 15 cm X 15 cm X 55 cm, notches of 1.5 cm, 3 cm, and 6 cm length were made, while in specimens 10 cm X 10 cm X 40 cm, notches of 3 cm and 5 cm length were made. Therefore, the ratios of notch depth to beam depth were 0.1, 0.2, 0.3, 0.4, and 0.5.

To compare with analytical results on crack propagation, monitoring of crack propagation was carried out in experiments. An experimental set-up is shown in Fig. 1. Four-point-bending tests were carried out.

* Department of Civil Engineering, Kumamoto University.
** Japan Highway Public Corporation.

Table 1 Mix proportions and material properties

	Unit weight (kg/m^3)					Averaged strength (kg/cm^2)	
	W	C	S	G		σ_c:comp.	σ_t:tensile
AE1	201	347	810	1083	-	297	34.1
AE2	201	347	810	542	542	299	34.5
SFR	181	347	742	536	536	433	45.5
MO	349	582	1164	-	-	278	27.1

The figure shows the case of non-symmetric loading. To determine critical stress intensity factors, load P was applied symmetrically. During experiments, AE events were monitored by using acoustic emission (AE) devices consisting of AE transducer (905S), a pre-amplifier, a discriminator, and a counter. The amplification was 60 dB gain in total and a bandpass filter 1 kHz to 300 kHz was employed. The threshold level for counting was set at 200 mV. Crack propagation was visually recorded by a video recorder.

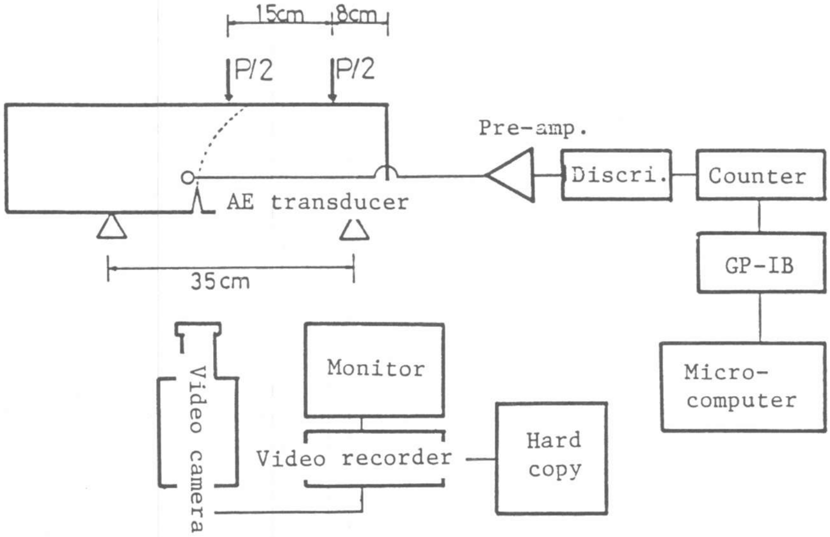

Fig. 1 Experimental set-up.

3. ANALYSIS

In the BEM formulation, the fundamental solution U_{ij} and the associated traction T_{ij} are utilized. It is assumed that a body consists of a regular surface S and a crack surface C. Then, a boundary integral equation for point x on S is presented, as follows;

$$cu_i(x) = \int_{S+C} (U_{ij}(x,y)t_j(y) - T_{ij}(x,y)u_j(y))ds, \tag{1}$$

where c is the configuration coefficient, which is equal to 1/2 in the smooth surface. $t_j(y)$ and $u_j(y)$ are a traction and a displacement on the boundary S+C.

An ideal crack configuration involves a surface discontinuity. Because two coplanar surfaces present an ill-posed problem, Eq. 1 becomes singular. To overcome this problem, the multi-region modelling approach (2) was adopted. A model in the numerical analysis is shown in Fig. 2. The upper figure shows the model in the first step of BEM analysis. Eq. 1 was formulated for regions on either side of the crack, and was stitched together with the displacement continuity and traction equilibrium conditions along the uncracked interface.

A stress intensity factor based on linear elastic fracture mechanics has been determined by a number of strategies in the BEM analysis. For a straight crack, the variation of displacements and stresses around a crack tip can be modelled by a crack element, which is an isoparametric element of quatratic shape functions with shifting the mid-point node to the quarter-point. For the regular boundary and the stitching interface, isoparametric elements with the mid-point node (conforming element) were utilized. Two crack elements were inserted at the notch tip as shown in the bottom of Fig. 2.

To calculate stress intensity factors from relative displacements at nodes on crack elements, one-point formulae by Smith (4) were adopted. It means the stress intensity factors were determined from displacements at the quarter-points.

The analysis of crack propagation in the arbitrary direction is based on the hypothesis that a crack grows in the direction perpendicular to the largest tensile stress at a crack tip (3). A relationship between angle and stress intensity factors is obtained, as follows;

$$K_I \sin\theta + K_{II}(3\cos\theta - 1) = 0, \qquad (2)$$

where K_I is the stress intensity factor of opening crack mode and K_{II} is that of in-plane shearing mode. In the first step, the interface

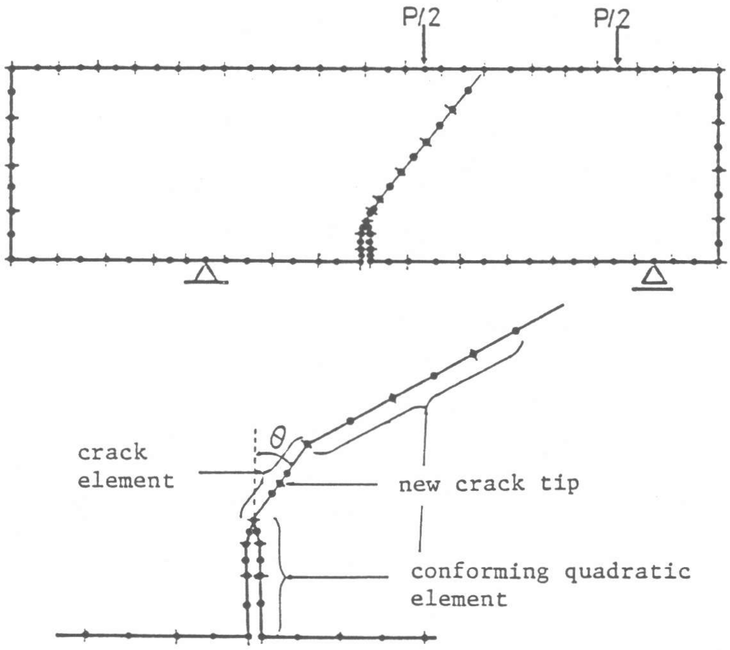

Fig. 2 Analytical model.

boundary was taken to lie along a possible path, and stress intensity factors K_I and K_{II} at a notch tip were computed. The angle θ of crack elements in the next step was obtained from Eq. 2. Then, the stitching interface was made from a new crack tip to a boundary point on the top surface. Here, the length of the crack element was set to 1 cm.

As the mechanical criterion of crack propagation, the critical value K_{Ic} was employed. In the case that K_I was larger than K_{Ic}, external load P was decreased up to the state : $K_I = K_{Ic}$ and new crack elements were created in the direction as shown in the bottom of Fig. 2. In the case that K_I at a notch tip was smaller than K_{Ic}, external load P was increased up to K_{Ic}. This procedure was successively repeated up to the final failure.

4. RESULTS AND DISCUSSION

Critical stress intensity factor of opening mode K_{Ic} was not determined by the conventional method, but by the method previously proposed (5). It is stated, as follow; In the four-point-bending tests of symmetric loading, the generation of AE events was monitored. Just

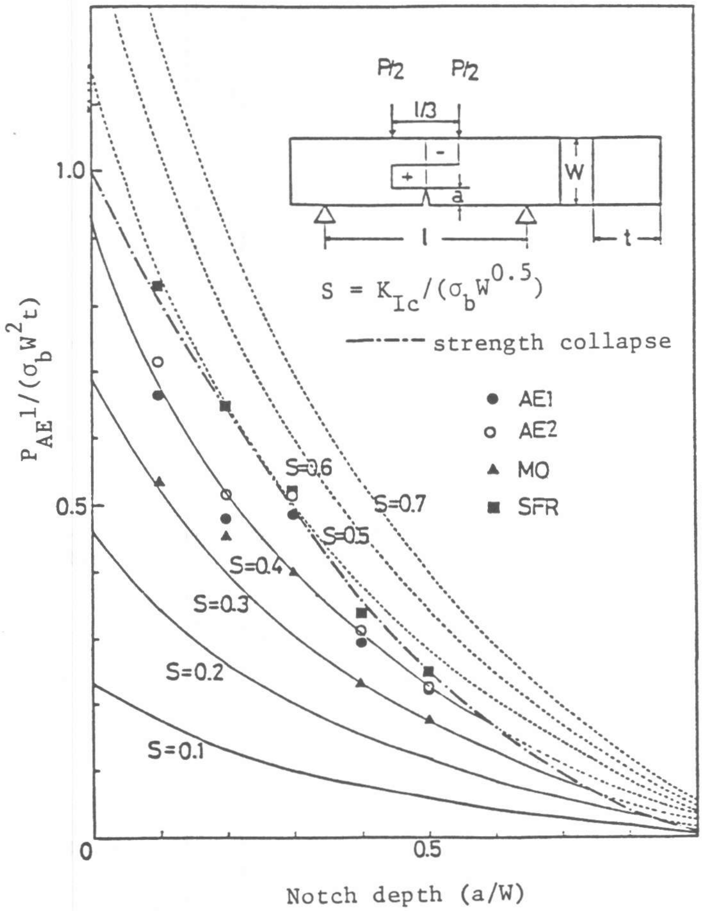

Fig. 3 P_{AE} and notch depth.

Table 2 Critical stress intensity factor K_{Ic} ($kg/cm^{1.5}$)

a/W	0.1	0.2	0.3	0.4	0.5	Average
AE1	65.0	64.2	69.3	65.5	68.2	66.4
AE2	69.3	68.4	73.1	70.8	69.0	70.1
SFR	106.0	113.0	98.5	99.4	99.8	103.3
MO	41.8	48.6	46.4	41.8	44.9	44.7

prior to the final failure, AE occurnce suddenly increased due to the initiation of unstable failure. This load level is referred to as P_{AE}. Load P_{AE} was applied to the model in the BEM analysis for determining the critical value K_{Ic}. The analysis was carried out by taking into account the exact configuration of tested specimens, including the notch configuration. Results of K_{Ic} values in all specimens were summarized in Table 2. In each case of notch depth, three specimens were tested and an averaged value is shown in the table. Although K_{Ic} values obtained by the conventional method is known as sensitive to notch depth, these values are fairly independent of the notch depth. Therefore, K_{Ic} values in all specimens were determined as the average of all cases of notch depth. They were utilized in the numerical analysis as the mechanical criterion for crack propagation.

Fig. 3 shows relationships between loads of collapse and notch depths in experiments. Following to Carpinteri (6), in the region below a curve of strength collapse, collapse due to crack propagation is dominant and K_{Ic} value is known free from the size effect. Relations of P_{AE} versus notch depth are plotted in the same figure. All points are located below the curve of strength collapse. It confirms that load P_{AE} is independent of the size effect.

Analytical results of crack propagation were compared with crack traces obtained by the video recorder. As an example, the result in AE1

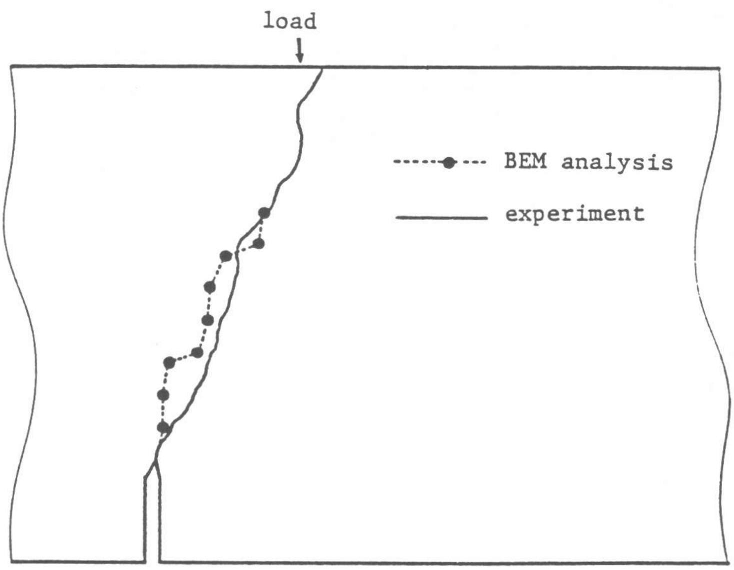

Fig. 4 A result of crack propagation (AE1).

specimen is shown in Fig. 4. Since the length of a crack element was fixed, crack propagates not smoothly but irregularly in the analysis. Cracks traced by the video recorder are shown by a solid curve. A reasonable agreement is observed. In other specimens, similar results were obtained, although the discrepancy between the analysis and the experiment was the largest in SFR specimen. As material properties, only Young's modulus and Poisson's ratio were taken into consideration in the analysis. It implies that the effect of reinforcement due to fiber was not exactly evaluated. Further improvement is required for applying the procedure to practical problems.

5. CONCLUSION

Crack propagation in concrete is investigated, on the basis of linear elastic fracture mechanics and the BEM analysis. As the mechanical criterion for crack initiation, the critical stress intensity factor determined from AE observation and the BEM analysis was employed. The process of crack propagation in the arbitrary direction was analyzed. Crack behaviors in the analysis were in good agreement with those obtained in experiments. These results confirm the usufulness of the BEM analysis for simulating crack propagation in concrete.

REFERENCES

(1) Mihashi, H.,"Survey of Fracture Mechanics of Concrete," Concrete Journal, JCI, Vol. 25, No. 2, 1987, pp. 14-25.
(2) Cruse, T. A. and Polch, E. Z.,"BEM for Fracture Mechanics Analysis," Proc. of BEM Symposium, JASCOM, Dec. 1986, pp. 111-133.
(3) Erdogan, F. and Sih, G. C.,"On the Crack Extension in Plates under Plane Loading and Transverse Shear," Journal of Basic Engineering, Transactions of ASME, Dec. 1963, pp. 519-527.
(4) Smith, R. N. L. and Mason, J. C.,"A Boundary Element Method for Curved Crack Problems in Two Dimensions," Boundary Element Methods in Engineering, eds. Brebbia, C. A., Springer-Verlag, 1982, pp. 472-484.
(5) Ohtsu, M.,"Nondestructive Evaluation of Cracks Based on Acoustic Emission," Transactions of JCI, Vol. 8, 1986, pp. 191-198.
(6) Carpinteri, A.,"Scale Effects in Fracture of Plain and Reinforced Concrete Structures," Fracture Mechanics of Concrete, eds. Sih, G. C. and Ditommaso, A., Martinus Nijhoff Publishers, 1985, pp. 95-140.